Supplemental Material for:

Title: GpsB promotes PASTA kinase signaling and cephalosporin resistance in *Enterococcus faecalis*

Authors: Nicole E. Minton, Dušanka Djorić, Jaime Little, Christopher J. Kristich

Running title: GpsB promotes signaling and cephalosporin resistance

Affiliation:

Department of Microbiology and Immunology

Center for Infectious Disease Research

Medical College of Wisconsin

8701 Watertown Plank Rd

Milwaukee, WI 53226

*For correspondence: ckristich@mcw.edu

Table S1. GpsB is specifically required for cephalosporin resistance.

	WT[b] MIC (μg/mL)[a]	Δ*gpsB* MIC (μg/mL)
Ceftriaxone	64	2
Cefuroxime	32	2
Ampicillin	0.5	0.5
Meropenem	2	1
Vancomycin	1	0.5
Bacitracin	32	32
Trimethoprim	0.25	0.125
Gentamicin	16	16
Chloramphenicol	4	4
Norfloxacin	2	2

[a] Minimal inhibitory concentrations (MIC) for ceftriaxone. Data represent the median MIC from 3 independent biological replicates.

[b] Strains analyzed were WT, OG1; and Δ*gpsB*, JL635.

Table S2. Complementation of the Δ*ireK gpsB* mutant strain.

Strain[b]	Ceftriaxone MIC (μg/mL)[a]
WT/vector	64
WT/p-*gpsB*-His	1024
Δ*ireK*/vector	1
Δ*ireK*/p-*gpsB*-His	1
Δ*ireK gpsB*/vector	0.5
Δ*ireK gpsB*/p-*gpsB*-His	2

[a] Minimal inhibitory concentrations (MIC) for ceftriaxone. Data represent the median MIC at least 2 independent biological replicates.

[b] Strains analyzed were WT/vector, OG1/pJRG9; WT/p-*gpsB*-His, OG1/pNEM4; Δ*ireK*/vector, JL206/pJRG9; Δ*ireK*/p-*gpsB*-His, JL206/pNEM4; Δ*ireK gpsB*/vector, NM6/pJRG9; and Δ*ireK gpsB*/p-*gpsB*-His, NM6/pNEM4.

Table S3. Strains and plasmids used in this study.

Strain or plasmid	Description of genotype	Source or reference
STRAINS		
E. coli		

TOP10	Routine cloning host	Lab stock
DH5α	Routine cloning host	Lab stock
BL21 (DE3)	Protein overexpression host	Lab stock
Nico21 (DE3)	Protein overexpression host	Lab stock
E. faecalis		
OG1	Wild-type, original unmarked isolate	(1)
OG1RF	Spontaneous rifampicin- and fusidic acid-resistant derivative of OG1	(2)
JL635	OG1 Δ*gpsB* (ΔL4-N130)	This work
JL206	OG1 Δ*ireK*	(3)
BL102	OG1 *ireK K41R*	(3)
NM6	OG1 Δ*ireK gpsB*	This work
JL650	OG1 Δ*mltG* (ΔQ6-D452)	This work
CK125	OG1RF Δ(*ireP ireK)*	(4)
SB23	OG1 Δ*croR*	(5)
E. faecium		
1,141,733	Wild-type reference strain, clinical isolate	(6)
JL638	1141733 *ΔgpsB* (ΔY6-N133)	This work
PLASMIDS		
pJH086	*E. faecalis* allelic exchange vector (CmR); *pheS** counterselection	(7)
pJLL254	Δ$gpsB_{Efs}$ deletion allele in pJH086	This work
pJLL261	Δ$gpsB_{Efm}$ deletion allele in pJH086	This work
pJLL272	Δ$mltG_{Efs}$ deletion allele in pJH086	This work
pET28a::his_6-smt_3	*E. coli* protein expression vector (Kn^r) with SUMO cleavable his_6 tag	Brian Volkman Lab
pET28b	*E. coli* protein expression vector (Kn^r)	Novagen
pNEM23	pET28a::his_6-smt_3-*gpsB*	This work
pNEM24	pET28a::his_6-smt_3-*gpsB 8A*	This work
pNEM46	pET28a::his_6-smt_3-*gpsB ΔP114-F136*	This work
pCJK111	pET28b::his_6-*ireK-n*	(4)
pCJK142	pET28b::his_6-*ireK-n K41R*	(4)
pBDL133	pET28b::his_6-smt_3-*ireP*	(8)
pJRG9	*E. faecalis* expression vector, constitutive $P23_s$ promoter (Cm^r)	(5)
pNEM4	pJRG9::*gpsB*-His_6	This work
pNEM6	pJRG9::*gpsB ΔP114-F136*-His_6	This work
pNEM29	pJRG9::*gpsB 8A*-His_6	This work
pJLL47	pJRG9::*irePireK*-His_6	This work

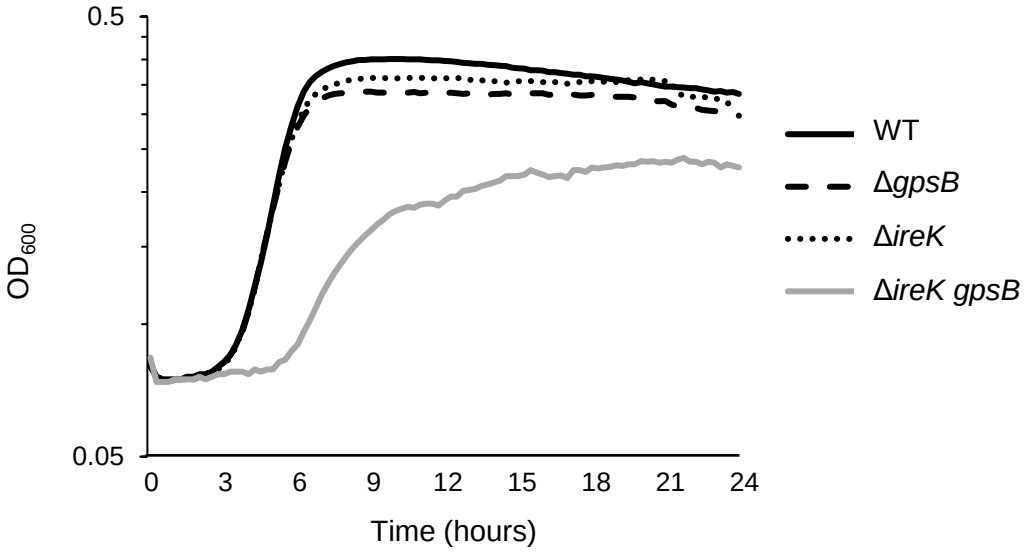

Figure S1. Growth phenotypes for various strains at 37°C. Cells were grown in Mueller-Hinton Broth for 24 hours at 37°C. The optical density at 600 nm (OD_{600}) was measured every 15 minutes. Data is representative of 3 biological replicates. Strains were wild-type (WT), OG1; Δ*gpsB*, JL635; Δ*ireK*, JL206; and Δ*ireK gpsB*, NM6.

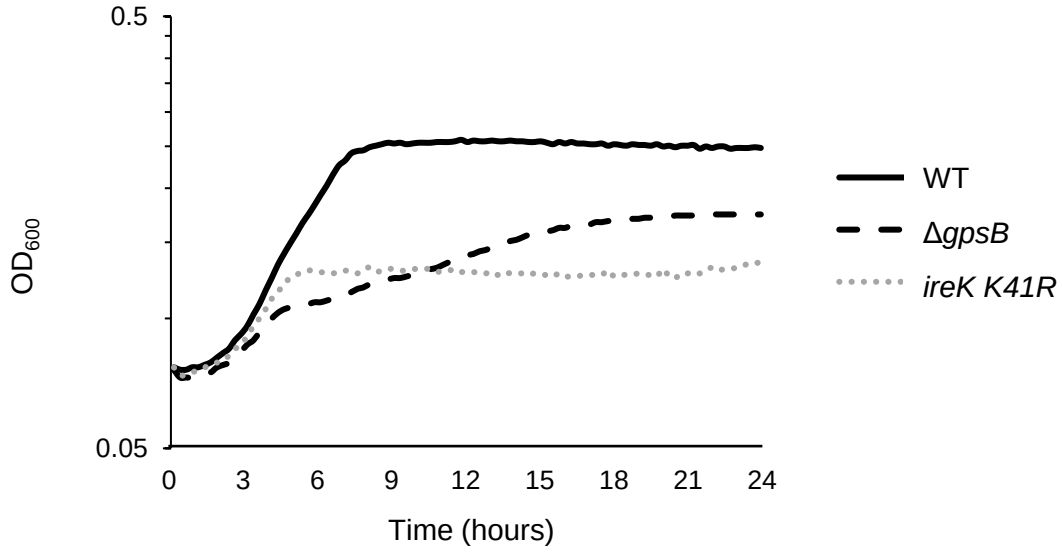

Figure S2. The Δ*gpsB* mutant exhibits a growth defect at 45°C. Cells were grown in Mueller-Hinton Broth for 24 hours at 45°C. The optical density at 600 nm (OD_{600}) was measured every 15 minutes. Data is representative of 3 biological replicates. Strains were wild-type (WT), OG1; Δ*gpsB*, JL635; and *ireK K41R*, BL102.

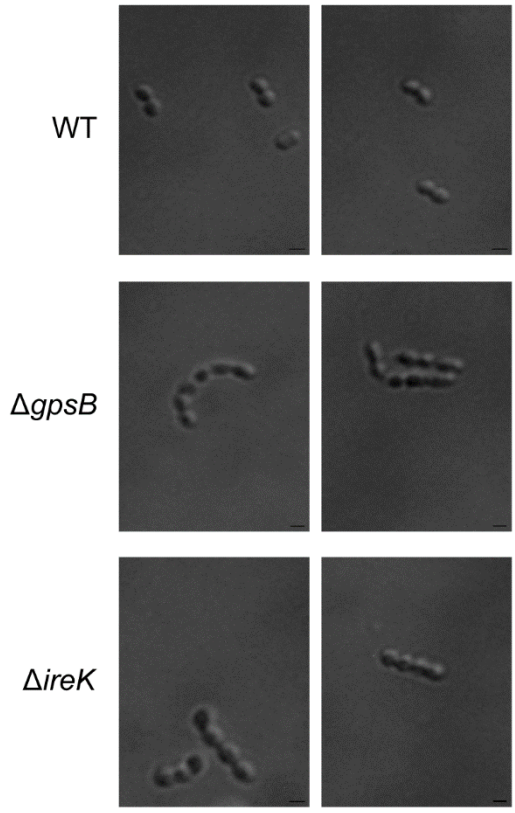

Figure S3. Δ*gpsB* cell morphology phenocopies Δ*ireK* cell morphology. Differential interference contrast microscopy was performed on stationary phase cultures grown in Mueller-Hinton Broth at 37°C. Scale bars represent 1 µm. Strains were wild-type, OG1; Δ*gpsB*, JL635; and Δ*ireK*, JL206.

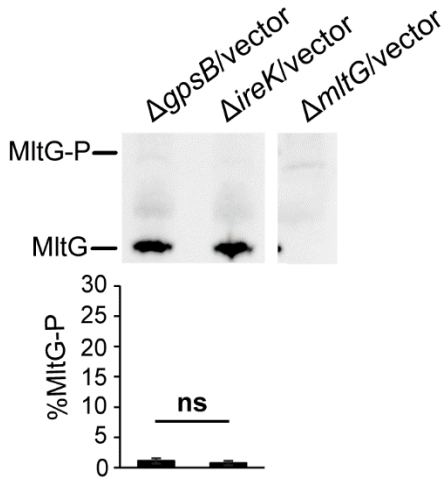

Figure S4. IreK signaling of the Δ*gpsB* and Δ*ireK* mutants are similar. Total protein lysates were prepared from exponentially-growing cells, and pairwise comparisons were subjected to Phos-tag SDS-PAGE followed by immunoblot analysis using antiserum to detect MltG. The immunoblot image is representative of at least 3 biological replicates per strain. Bar graph data show the average %MltG phosphorylation (% MltG-P) of the 3 replicates. Error bars represent one standard deviation. ns, not significant; student's T-test (heteroscedastic, two-tailed). Strains were Δ*gpsB*/vector, JL635/pJRG9; Δ*ireK*/vector, JL206/pJRG9; and Δ*mltG*/vector, JL650/pJRG9.

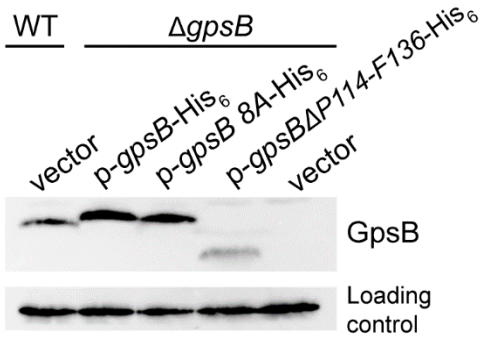

Figure S5. Immunoblot analysis of ectopically expressed wild-type GpsB and GpsB mutants. Total protein lysates were prepared from exponentially-growing *E. faecalis* cells harboring the vector or plasmids expressing wild-type or mutant GpsB-His_6. Immunoblotting was performed using antisera to detect GpsB and RpoA (loading control). Strains were WT/vector, OG1/pJRG9; Δ*gpsB*/p-*gpsB*-His_6, JL635/pNEM4; Δ*gpsB*/p-*gpsB 8A*-His_6, JL635/pNEM29; Δ*gpsB*/p-*gpsB ΔP114-F136*-His_6, JL635/pNEM6; and Δ*gpsB*/vector, JL635/pJRG9.

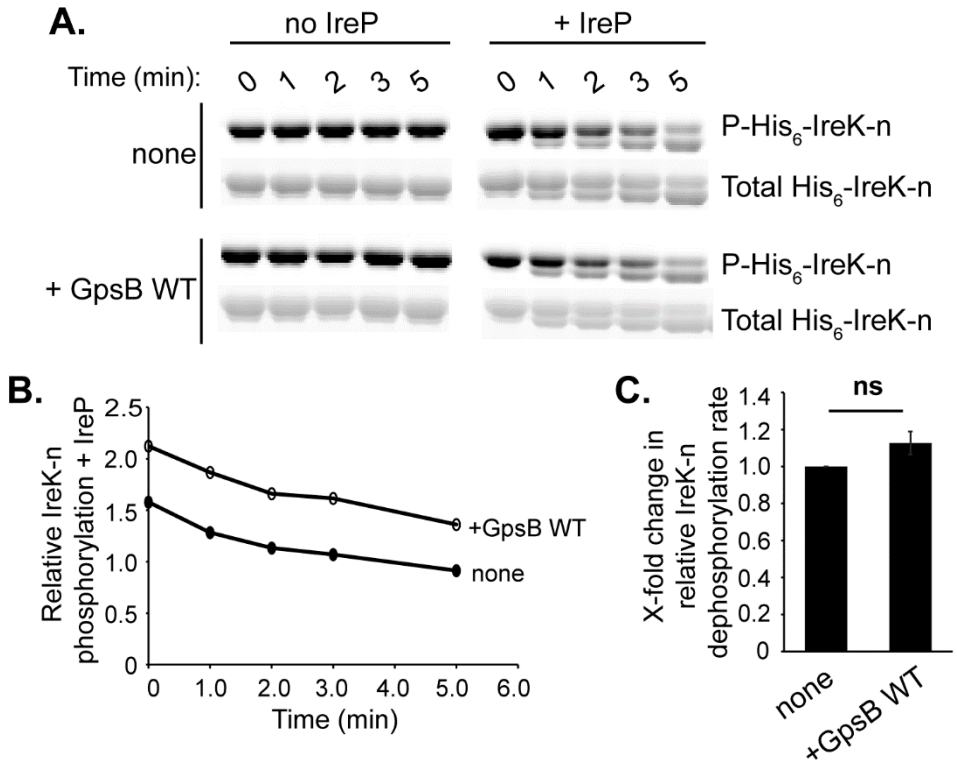

Figure S6. GpsB does not alter IreP-mediated dephosphorylation of IreK *in vitro*. *in vitro* dephosphorylation assays were performed with purified proteins to assess the impact of wild-type GpsB (GpsB WT) on IreK dephosphorylation. Phosphorylated His_6-IreK-n was incubated at room temperature with10-fold excess of wild-type GpsB relative to phosphorylated His_6-IreK-n. Samples were taken at various time intervals after the addition of IreP. **A.** After SDS-PAGE, Pro-Q Diamond phosphoprotein stain was used to visualize phosphorylated His_6-IreK-n (P- His_6-IreK-n) and SYPRO Ruby protein gel stain was used to visualize total His_6-IreK-n. Gel images are representative of two independent experiments. **B.** The phosphorylated His_6-IreK-n and total His_6-IreK-n signals from the gels were quantified. Relative His_6-IreK-n phosphorylation for each timepoint was calculated by determining the ratios of phosphorylated His_6-IreK-n to total His_6-IreK-n for each timepoint. The graph is representative of data from 2 independent experiments. **C.** Initial relative His_6-IreK-n phosphorylation rates were determined by finding the slopes of the best fit lines in graph (B) for each reaction. Shown are the x-fold-changes in rate for the reactions that contain GpsB relative to the reaction without GpsB. Data are the mean x-fold

change from 2 independent experiments. Error bars represent one standard deviation. ns = not significant, student's T-test (heteroscedastic, two-tailed).

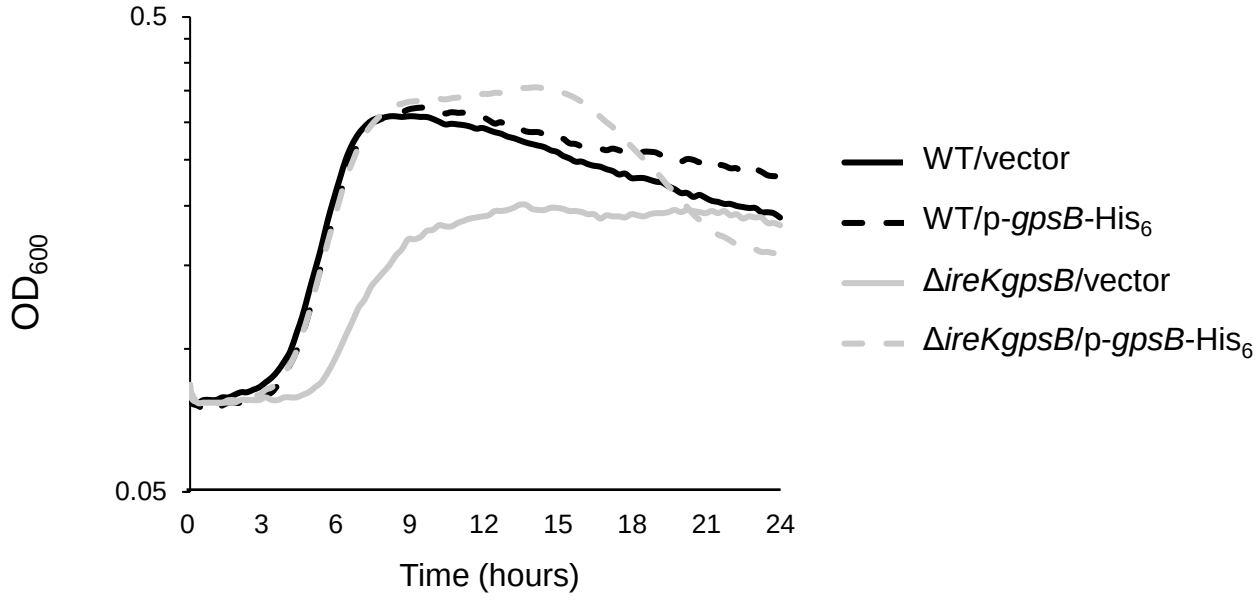

Figure S7. Ectopic expression of *gpsB* restores normal growth to the Δ*ireK gpsB* mutant. Cells were grown in Mueller-Hinton Broth for 24 hours at 37°C. The optical density at 600 nm (OD_{600}) was measured every 15 minutes. Data is representative of 3 biological replicates. Strains were wild-type (WT)/vector, OG1/pJRG9; WT/p-*gpsB*-His_6, OG1/pNEM4; Δ*ireK gpsB*/vector, NM6/pJRG9; and Δ*ireK gpsB*/p-*gpsB*-His_6, NM6/pNEM4.

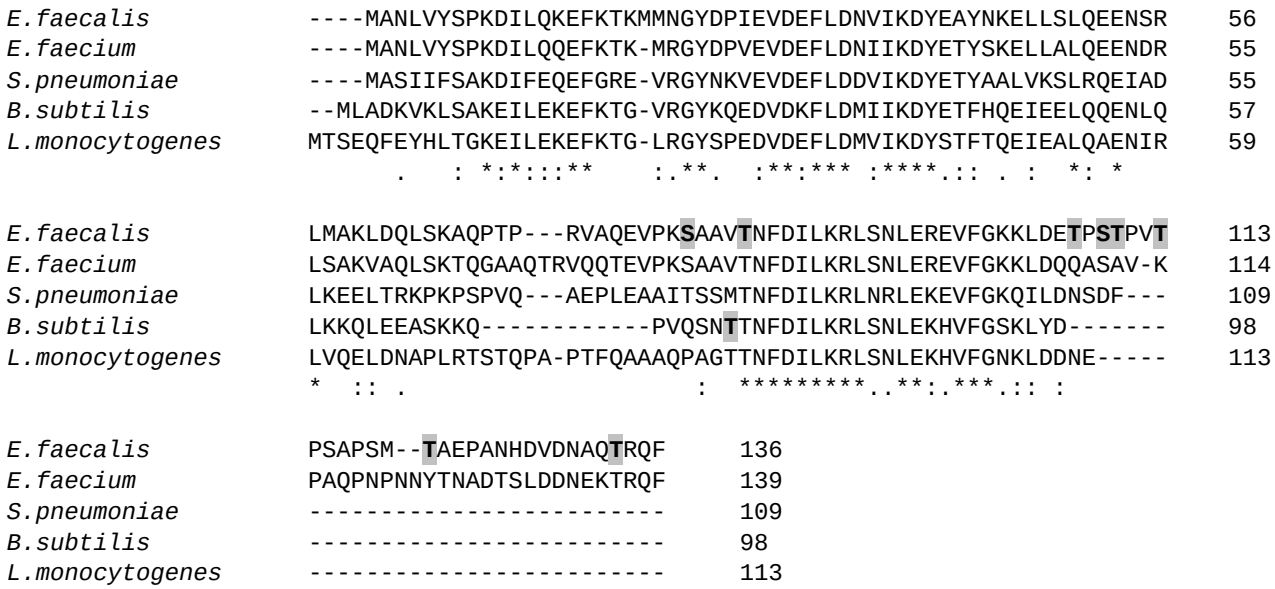

Figure S8. Sequence alignment of enterococcal GpsB with homologs from other bacterial species.

Sequences of GpsB homologs from various bacterial species were compared using Clustal Ω. Highlighted in grey are the putative phosphorylation sites for *E. faecalis* GpsB and the known phosphorylation site for *B. subtilis* GpsB. GpsB homologs represented are from *Enterococcus faecalis* OG1RF (WP_002357990.1), *Enterococcus faecium* 1,141,733 (WP_002309359.1), *Streptococcus pneumoniae* D39 (WP_000146522.1), *Bacillus subtilis* 168 (WP_003225629), *and Listeria monocytogenes* EDG-e (WP_003722998.1).

Supplemental References:

1. Gold OG, Jordan HV, van Houte J. 1975. The prevalence of enterococci in the human mouth and their pathogenicity in animal models. Arch Oral Biol 20:473-477.
2. Dunny GM, Brown BL, Clewell DB. 1978. Induced cell aggregation and mating in *Streptococcus faecalis*: evidence for a bacterial sex pheromone. Proc Natl Acad Sci U S A 75:3479-3483.
3. Labbe BD, Kristich CJ. 2017. Growth- and stress-induced PASTA kinase phosphorylation in *Enterococcus faecalis*. J Bacteriol 199:e00363-17.
4. Kristich CJ, Little JL, Hall CL, Hoff JS. 2011. Reciprocal regulation of cephalosporin resistance in *Enterococcus faecalis*. MBio 2:e00199-11.
5. Snyder H, Kellogg SL, Skarda LM, Little JL, Kristich CJ. 2014. Nutritional Control of Antibiotic Resistance via an Interface between the Phosphotransferase System and a Two-Component Signaling System. Antimicrob Agents Chemother 58:957-965.
6. Palmer KL, Carniol K, Manson JM, Heiman D, Shea T, Young S, Zeng Q, Gevers D, Feldgarden M, Birren B, Gilmore MS. 2010. High-quality draft genome sequences of 28 *Enterococcus* sp. isolates. J Bacteriol 192:2469-2470.
7. Kellogg SL, Little JL, Hoff JS, Kristich CJ. 2017. Requirement of the CroRS two-component system for resistance to cell wall-targeting antimicrobials in *Enterococcus faecium*. Antimicrob Agents Chemother 61:e02461-16.
8. Labbe BD, Hall CL, Kellogg SL, Chen Y, Koehn O, Pickrum AM, Mirza SP, Kristich CJ. 2019. Reciprocal regulation of PASTA kinase signaling by differential modification. J Bacteriol 201:e00016-19.